Osseous paleopathologies of *Bonapartesaurus rionegrensis* (Ornithopoda, Hadrosauridae) from Allen Formation (Upper Cretaceous) of Patagonia Argentina

Penélope CRUZADO-CABALLERO[1,2,3,4], Agustina LECUONA[2,3], Ignacio CERDA[2,3,5], Ignacio DÍAZ-MARTÍNEZ[2,3]

1 Área de Paleontología, Departamento de Biología Animal, Edafología y Geología, Universidad de La Laguna, Av. Astrofísico Francisco Sánchez s/n, 38200, San Cristóbal de La Laguna, Santa Cruz de Tenerife, Spain. pcruzado@ull.edu.es

2 Universidad Nacional de Río Negro. Instituto de Investigación en Paleobiología y Geología, Río Negro, Argentina.

3 IIPG. UNRN. Consejo Nacional de Investigaciones Científicas y Tecnológicas (CONICET). Av. Roca 1242, (R8332EXZ) General Roca, Río Negro, Argentina. alecuona@unrn.edu.ar, idiaz@unrn.edu.ar

4 Grupo Aragosaurus-IUCA, Departamento de Ciencias de la Tierra, Área de Paleontología, Universidad de Zaragoza, Zaragoza, Spain.

5 Museo Provincial "Carlos Ameghino", Belgrano 1700, Paraje Pichi Ruca (predio Marabunta), Cipolletti, Río Negro, Argentina. nachocerda6@gmail.com

Keywords: hadrosaurid, Gondwana, fracture, neoplasm, pathology

ABSTRACT

The paleopathological record provides relevant information about paleobiology and paleoecology of fossil organisms. Based on the information obtained from paleopathologies, it is possible to infer how these injuries affected inter- and intraspecific relationships among organisms, and their interaction with the environment. For instance, fractures and infections may affect their behavior, such as locomotion, strength, and stamina, leading in some cases to death. Here, we describe the injuries recorded in the hadrosaurid *Bonapartesaurus rionegrensis* and their possible implications in its paleobiology. Three pathologies have been identified, two in caudal vertebrae neural spines and the third in the left metatarsal II. The caudal vertebra MPCA-Pv SM2/17 presents a displaced fracture with an advanced stage of healing and probably related to a trauma. The caudal vertebra MPCA-Pv SM2/19 shows an almost fully healed fracture produced by an impact or stress event. Finally, in the metatarsal II there is an overgrowth of pathological bone that covers the shaft interpreted as probably a neoplasm probably a neoplasm (e.g., osteosarcoma). The suite of vertebral paleopathologies would have generated pain and discomfort during its daily activity.

1. INTRODUCTION

Studies in paleopathology provide valuable information about the historical record of the injuries and how they have affected the paleobiology and paleoecology of organisms (Rothschild, 2009; Arbour and Currie, 2011; Rothschild et al., 2012; Peterson and Vittore, 2012; Tanke and Rothschild, 2014; Kappelman et al., 2016; Dumbravă et al., 2016; Hearn and Williams 2019 and references therein). Trauma and paleopathologic records are abundant in Mesozoic dinosaur bones, such as in theropods, sauropods and ornithopods (see Cruzado-Caballero et al., 2020 and references therein).

Hadrosauridae is one of the most abundant and diverse clade of Late Cretaceous ornithopod dinosaurs in the Northern Hemisphere. They have one of the richest fossil record of this time span and region, that includes mummies, ontogenetic series, eggs and nests, skin impressions, and footprints (Horner and Currie, 1994; Horner et al., 2004; Murphy et al., 2006; Farke et al., 2013; Bell et al., 2014; Díaz-Martínez et al., 2015). This fossil record also accounts for abundant remains with pathologies and trauma present in both bones and skin (Rothschild and Tanke, 2006; Straight et al., 2009; De Palma et al., 2013; Tanke and Rothschild, 2014; Anné et al., 2015, 2016; Dumbravă et al., 2016; Matthias et al., 2016; Ramírez-Velasco et al., 2017). The hadrosaurid record in Gondwana is less known, mainly coming from Patagonia Argentina. Four species have been considered valid from this region, *Secernosaurus koerneri* Brett-Surman, 1979, *'Kritosaurus' australis* Bonaparte, Franchi, Powell and Sepulveda 1984, *Lapampasaurus cholinoi* Coria, González Riga and Casadio, 2012, *Bonapartesaurus rionegrensis* Cruzado-Caballero and Powell, 2017, and diverse cranial, postcranial and ichnological remains of indeterminate hadrosaurids (Cruzado-Caballero, 2017; Díaz-Martínez et al., 2016). Among those species, *Bonapartesaurus* presents pathological neural spines in two caudal vertebrae and a pathological second left metatarsal, representing the first South American hadrosaurid found with pathologies.

The main goal of the present contribution is to describe in detail the pathologies present in the neural spines of the two caudal vertebrae (MPCA-Pv SM2/17 and MPCA-Pv SM2/19) and the metatarsal II of the almost complete left foot (MPCA-Pv SM2/60-69) of *Bonapartesaurus rionegrensis* holotype (MPCA-Pv SM2). Additionally, we attempt to elucidate the putative causes of these injuries and the impact they may have had in the paleobiology of this hadrosaurid.

2. MATERIAL AND METHODS

The studied material correspond to the hadrosaurine hadrosaurid *Bonapartesaurus rionegrensis* accessed at the Museo Provincial "Carlos Ameghino" (MPCA) in Cipolletti (Río Negro, Argentina). This specimen was collected by Jaime Powell in 1984 from the Salitral Moreno site, General Roca (Río Negro, Northern Patagonia, Argentina; Fig. 1; Powell, 1987), proceeding from the deposits of the Allen Formation (upper Campanian–lower Maastrichtian, Cruzado-Caballero and Powell, 2017). The Salitral Moreno locality was discovered by Prof. Roberto Abel (former director of Museo Provincial "Carlos Ameghino") in 1983 (Powell, 2003). The first systematic exploration began during 1984, when several vertebrates and plants remains were collected (Powell, 2003). All the postcranial skeletal elements from the holotype of *Bonapartesaurus rionegrensis* (MPCA-Pv SM2) have been macroscopically examined and pathological features have been recognized. The pathologies are present in three bony structures, the neural spines of two middle caudal vertebrae (MPCA-Pv SM2/17 and MPCA-Pv SM2/19; Fig. 2A-F) and the shaft of the second metatarsal of the almost complete and articulated left pes (MPCA-Pv SM2/60-69; Fig. 2G-H).

Regarding non-avian dinosaurs, the most important discoveries from Salitral Moreno locality includes the titanosaur *Rocasaurus muniozi* Salgado and Azpilicueta, 2000*,* the hadrosaurid *Bonapartesaurus rionegrensis* and the first definitive evidence of ankylosaur dinosaurs (see García and Salgado, 2013 for a review).

2.1. CT Scan

All bones were CT Scanned using axial computed tomography, with a Phillips Brillance model at Diagnósticos Gamma Medical Centre of San Miguel de Tucumán, Tucumán Province (Argentina). Settings for differential diagnosis of bone pathologies were used (vertebrae: 120 kv and 219 mA with 0.8 slice thickness; pes: 120 kv and 76 mA with 0.75 slice thickness). All CT Scan images were saved in DICOM format images, and analyzed with 3D Slicer (v. 4.10.2) and ImageJ (v. 1.52p) softwares.

The pes has some matrix remains and a large block of plaster with a metallic bar inside below the fossil, originally made to maintain the relative position of bones. The significant thickness of the complete block (MPCA-Pv SM2/60-69), the high density of matrix and plaster, and the presence of this metallic bar, caused many noise in the acquisition of the CT images and prevented the observation and recognition of some details (Fig. 5B). However, this noise did not prevent the examination and characterization of the important structural features of the pathology.

2.2. Paleohistology

In order to analyze the microscopic features of the pathological tissue found in the metatarsal II of *Bonapartesaurus rionegrensis*, a histological thin-section was conducted. The sample was taken from the distal portion of the pathological structure and performing a transversal thin-section. A complete transversal section of the metatarsal shaft cannot be made due to the inclusion of the articulated pes within the matrix and plaster. The sample included not only part of the pathological tissue but also part of the underlying non-pathological cortex. Histological thin-sections were performed by one of us (IAC) in the Paleohistological Laboratory of the Museo Provincial "Carlos Ameghino" (Cipolletti, Río Negro Province, Argentina) using standard methods (Chinsamy and Raath, 1992; Cerda et al., 2020). The samples were examined with a petrographic polarizing microscope (BestScope and Nikon E200 POL). The histological nomenclature and definitions applied in the present study are based on Francillon-Vieillot et al. (1990) and de Ricqlès et al. (1991).

3. DESCRIPTION

3.1. Caudal vertebra MPCA-Pv SM2/17

The pathological tissue of this vertebra is located approximately at mid-height of the neural spine, coinciding with a marked curvature of the sagittal axis toward the right side (Fig. 2A-B, E, and Fig. 3). The lateromedial diameter of the wider pathological region is 33 mm, contrasting with the 29 mm of the healthy spines of the same individual. The entire subperiosteal surface of the callus has a rough texture with irregular and shallow depressions due to the surface defects lesions (Fig. 2E).

There is a white area with irregular width, distributed through most of the neural spine, being larger than the typical for compact bones, thus probably corresponding to the resins used to fill taphonomic fractures (Fig. 3C-F). There is an area with a grey color similar to cancellous tissue of the healthy bone (Fig. 3C-F). In the pathologic area, there is a cavity, observed as a black region in the several successive images of the CT-scan (Fig. 3E).

3.2. Caudal vertebra MPCA-Pv SM2/19

MPCA-Pv SM2/19 shows a large pathological ball-shaped overgrowth at mid height of the neural spine (Fig. 2C-D, F). The pathological area increases considerably the mediolateral width (41 mm) of the axis compared to the non-pathological elements (29 mm). The subperiosteal surface has a coarse appearance (Fig. 2F) similar to MPCA-Pv SM2/17; but, unlike this one, the neural spine is straight, lacking the lateral displacement and curvature.

The CT Scan images show the cancellous tissue as a grey area (Fig. 4B), similar to MPCA-Pv SM2/17. There is a periosteal reaction observed by a lucid sheath that surrounds the original cortex and merges with it. It can also be observed several white areas corresponding to the resin used during the preparation of the material (Fig. 4C-E).

3.3. Pes MPCA-Pv SM2/60-69

The metatarsal II presents a considerable overgrowth of pathological bone that covers the shaft of the element, in about two-thirds of the complete length of the bone (Fig. 2G-H). The pathology notably increases the mediolateral width of the shaft (77 mm) compared to the non-pathological elements (57 mm in metatarsal III, 53 mm in metatarsal IV), and the medial surface of the overgrowth almost reaches the same width as the proximal and distal articular surfaces. The periosteal reaction of the tissue does not reach the ends of the metatarsal, which maintain their original shape and texture. The subperiosteal surface has a rugose appearance, covered with shallow and irregular pits(Fig. 2H), and lacking a cloaca on the outer surface for drainage of pus.

A clear observation of the CT Scan images was not possible due to the presence of the metallic bar mentioned above (Fig. 5B), however, several pathological features were recognized. In antero-dorsal view, a reduction in bone density can be identified throughout the diaphysis below the periosteal reaction tissue of the metatarsal II (Fig. 5B-C). In transversal view, it is observed a non-uniform distribution of the periosteal reaction, being larger in the lateral and dorsal regions, having a small development in the ventral region, and lacking any callused area in the medial side (Fig. 5D-I). Several areas of cortical destruction are also observed, which are more prominent proximally, associated with a wide transitional zone to normal bone (Fig. 5 D-F). The transversal section of the distal region, shows an osseous tissue outburst through the cortex (Fig. 5 G-I).

The histological thin-section shows two distinct areas, a pathological and a non-pathological one (Fig. 6A). The pathological region occupies the external half of the sample and is more porous than the underlying non-pathological cortex. At microstructural level, the pathological tissue includes both primary and secondary bone tissues. The primary bone consists of a highly vascularized matrix in which intrinsic fibers exhibit a rather chaotic spatial arrangement (Fig. 6B-D), osteocyte lacunae are extremely abundant, however, their original size and shape appears to be strongly altered by diagenetic processes. Primary vascular canals have mostly a longitudinal arrangement. The high porosity of the pathological bone is mostly due to the presence of abundant resorption cavities (Fig. 6E-F), which size and shape is strongly variable, forming in some areas a rather cancellous structure. These cavities are usually coated by secondarily deposited lamellar bone tissue (Fig. 6F). The underlying, non-pathological cortex is mostly formed by dense Haversian bone tissue (Fig. 6G-H). The size and shape of the secondary osteons is rather variable. Scarce remains of primary bone tissue appear to be parallel fibered bone, which are only present near the transition between pathological and non-pathological cortices.

4. PATHOLOGICAL DIAGNOSES

Bonapartesaurus rionegrensis has three pathological elements, which present fractures with amorphous masses of bone (a callus tissue) and elliptical erosions associated to the amorphous mass, tentatively identified as infections.

4.1. Fractures

According to Mahajan et al. (2015) a fracture is a disruption in the continuity of the bone with or without displacement of the fragments. It is also associated with soft tissue damage, broken blood vessels, lacerated periosteum, and bruised muscles and nerves. They can be classified as traumatic or atraumatic, the latter including pathologic, based on the health condition of the bones before the fracture. Traumatic fractures result from a force applied to the bone, whereas the atraumatic pathologic fractures are the result of a reduction in the bone strength caused by a regional lesion or disease that affects the bone structure and reduces its resistance to normal stresses (Mahajan et al., 2015). The properties of the force (e.g., magnitude, direction, loading rate, how long it was applied) and the characteristics of the bone where the force is applied (e.g., density, fatigue strength, resilience, elasticity; Rothschild and Martin, 2006) are factors that strongly affect the magnitude of the traumatic fractures. By varying the amount and relationship among these factors they will result in different types of fractures, such as oblique (closed or displaced), transverse, greenstick, spiral, compression, impact, and stress fractures (Rothschild and Martin, 2006). On the other hand, pathologic fractures are characterized by the occurrence in bone that already have a tumor, necrosis, osteomyelitis, or parasitic disease (Mahajan et al., 2015). Bone fractures are common in the dinosaur fossil record, having been found in sauropodomophs (e.g., Rothschild and Molnar, 2005, Hao et al., 2020), theropods (e.g., Rothschild and Martin, 2006, Anné et al., 2015), neoornithischians (e.g., Rothschild and Martin, 2006, Hedrick et al., 2016, Cruzado-Caballero et al., 2020), and thyreophorans (e.g., Arbour and Currie, 2011, Hao et al., 2020).

4.2. Infections

Infection diseases are due to the invasion and proliferation of pathogens (e.g., bacteria, parasites) in an organism body, which produce inflammation, pain, and sometimes infection of the affected tissues (Jacobson, 2007). When the infection affects the bone is called osteitis (i.e., inflammation of the bone) or osteomyelitis (i.e., inflammation of bone marrow; Anné et al., 2015). Infections are not very common in dinosaur fossil record, and many of them have been diagnosed as osteomyelitis (Hanna, 2002; Rothschild and Martin, 2006; Peterson and Vittore, 2012; Ramírez-Velasco et al., 2017; Clayton, 2018). They are even unusual cases of multiple infections in the same individual (Hanna, 2002; Lu et al., 2017; Tanke and Rothschild, 2014; García et al., 2016; Hunt et al., 2019). Osteomyelitis, in a mammalian immune system model, can be classified as pyogenic (suppurative), if the infection has pus production; or nonpyogenic (non-suppurative), without pus production (Hanna, 2002; Rothschild and Martin, 2006). In this model, they can develop as an acute response (a new infection), subacute (caused by an open wound), and chronic (a recurring infection; Hanna, 2002; Rothschild and Martin, 2006; Clayton, 2018). Acute and subacute cases of osteomyelitis cause periosteal reaction, cortical irregularity, and demineralization, whereas chronic cases include thick, sclerotic, irregular bone, and a swollen periosteal surface (Resnick and Niwayama, 1981). By contrast, in a reptilian immune system model response (including birds), small fibrin cysts (fibrisces) would form at the origin of infection, which would tend to calcify in advanced stages (Montali, 1988; Gomis et al., 1997; Huchzermeyer and Cooper, 2000; Cooper, 2005; Rega, 2012; Foth et al., 2015).

A possible cause of an osteomyelitis is a trauma that affects soft tissue or bone, producing an open wound through which pathogens enter and they may spread through the bloodstream (Hanna, 2002; Peterson and Vittore, 2012). This type of infection is not very frequent in the dinosaur fossil record, however it has been reported in all dinosaurian groups, such as basal sauropodomorphs (Xing et al., 2018), sauropods (García et al., 2016; Clayton, 2018), theropods (Hanna, 2002; Bell and Coria, 2013; Xing et al., 2013; Foth et al., 2015; Hone and Tanke, 2015; Senter and Juengst, 2016), pachycephalosaurids (Peterson and Vittore, 2012), ankylosaurids (Arbour and Curie, 2011), stegosaurids (McWhinney et al., 2001), ceratopsids (Tanke and Farke, 2006), and ornithopods (Anné et al., 2015; Tanke and Rosthchild, 2014; Ramirez-Velasco et al., 2017; Hunt et al., 2019).

4.3. Neoplasms

A neoplasm, or tumor, is an abnormal proliferation of cells resulting from errors in the cell division regulation (Alberts et al., 2019; Pierce, 2019; de Sousa et al., 2020). According to Rothschild and Martin (2006), in order to recognize a neoplasia (tumor) in a bone, or a tumor-like disorder, an analysis of the pattern of bone destruction, nature, and extent of medullary, cortical or periosteal reaction or disruption, as wells as the calcification of the matrix of the tumor is mandatory. If the neoplasms are slow growing, do not invade other tissues, and do not produce metastases, they are considered as benign, such as osteoma, condroma, osteochondroma, histiocytoma, hemangioma, fibroma, odontoma (Chhem and Brothwell, 2008). Conversely, when neoplasms have a constant destructive growth, are usually very invasive, and expansive, they are considered as malignant, such as an osteosarcoma, chondrosarcoma, and hemangiosarcoma (Chhem and Brothwell, 2008; De Boer et al., 2013; Alberts et al., 2019; Pierce, 2019; de Sousa et al., 2020).

These diseases are found in almost all metazoans (Aktipis et al., 2015) and have an extensive fossil record in vertebrates (see references in de Sousa et al., 2020). Among dinosaurs, they have been described more abundantly in hadrosaurids, although they have also been found in other dinosaurs (Rothschild et al., 2003; de Sousa et al., 2016; Jentgen-Ceschino et al., 2020).

4.4. Caudal vertebra MPCA-Pv SM2/17

The presence of an area of bony overgrow, a slight lateral displacement of the distal fragment of the neural spine, and the curvature of its main axis, suggest that the fracture was caused by a trauma. However, this fracture could not be identified in the tomographic images due to the presence of taphonomic breaks that masked it. The deviation of the long axis of the neural spine is consistent with an impact resulted from a traumatic event (Foth et al., 2015).

4.5. Caudal vertebra MPCA-Pv SM2/19

The presence of a noticeable and well-developed area of bony overgrow; suggest the presence of a fracture. As mentioned before, the rough and irregular periosteal surface is common in fractured bones and it can be an indicator of an infection (Rothschild and Martin, 2006).

4.6. Pes MPCA-Pv SM2/60-69

The metatarsal II shows a reduction in bone density, as well as several regions of cortical destruction, observed on the CT-scan images;. All these features suggest the presence of a neoplasm (Rothschild and Martin, 2006).

5. PALEOBIOLOGICAL IMPLICATIONS

In order to hypothesize possible functional changes in *Bonapartesaurus* that could have affected its paleoecology, paleobiology, and functional behavior, it is important to infer the muscles, ligaments and other soft tissues that attach to the regions affected. Reconstructing the attachment sites in fossil animals is sometimes hard and more or less speculative. It depends not only in having closely related living relatives on which be able to see the muscles, but also the osteological correlates on the studied fossil (Bryant and Russell, 1992; Witmer, 1995, 1997). Many paleontologists have attempted to infer the muscles in fossil vertebrates, and particularly focused in mammals and dinosaurs (e.g., Tarsitano, 1981; Carrano and Hutchinson, 2002; Dilkes, 2000; Dumbravă et al., 2013; Norman, 1986; Schachner et al., 2011, 2020; Siviero et al., 2020).

5.1. Fractures in the caudal vertebrae and inferences in tail movement

In the hadrosaurid fossil record, the lesions in the tail elements are very common (Tanke and Rothschild, 2014; Siviero et al., 2020). Lesions in the tail are usually found in adults more than in juveniles, and they have been identified as fractures, spinal osteomyelitis, congenital deformities, spondyloarthropathies, and/or neoplasms (Ramirez-Velasco et al., 2017; Tanke and Rothschild, 2014). The fractures are commonly located at or near the tip of the neural spine, and they can represent a healed fracture as observed in the neural spines of MPCA-Pv SM2/17 and MPCA-Pv SM2/19, respectively.

The occurrence of both pathological caudal vertebrae of *Bonapartesaurus* in the middle region of the tail is consistent with the interpretation of hadrosaurids having flexible and vulnerable middle to posterior region of the tail (Siviero et al., 2020). Hadrosaurids tail have moderate size epaxial muscles and large size hypaxial ones (Persons and Currie, 2014), where the major component of the latter is the *caudofemoralis* muscle, which tappers posteriorly reaching the middle of the tail (Siviero et al., 2020). The presence of this large muscle, combined with the presence of ossified tendons in the anterior half region of the tail, made the anterior region highly mechanically stable (Siviero et al., 2020). Conversely, from the middle to posterior region of the tail, the absence of such a strong hypaxial musculature and absence of ossified tendons, made the tail more flexible and prone to mechanical stress and trauma (Siviero et al., 2020).

This type of pathology in caudal vertebrae have been often described as due to accidental bumps against inanimate objects or knocks due to intraspecific encounters (e.g., mating trauma, trampling or aggressive interactions with conspecifics) or interspecific ones (e.g., defense against predator), whether accidental or driven by interactive behaviors (Horner et al., 2004; Tanke and Rothschild, 2014). A recent new interpretation has been proposed, where the breakage of the neural spine can occur by mechanical stress (Siviero et al., 2020).

In *Bonapartesaurus*, the affected vertebrae are from the middle region of the tail and, although they are close to each other, there is another vertebra between them without apparent pathologies. The degree of healing of the fractures, and the degree of development of the infections are different in each neural spine, thus it is not possible to elucidate if both injuries occurred in one or two independent events. The cause of both fractures could be a trampling, a hit with an object, an intraspecific interaction due to gregarious behavior, defense against a predator attack or simply due to running stress (Siviero et al., 2020), these are all good hypothesis, but we cannot determine which one is more likely.

5.2. Neoplasm in metatarsal II and inferences for foot movement

Lesions in appendicular bones are common in the hadrosaurid fossil record (Tanke and Rothschild, 2014). The type of injury they present may potentially be lethal and/or have implications for the animal behavior, and thus impacting in its interaction with other animals and the environment, and its survival abilities (Tanke and Rothschild, 2014; Cruzado-Caballero et al., 2020).

The pathologic injury of metatarsal II of *Bonapartesaurus* is interpreted as a tumor. In order to analyze the potential effect in its pedal and limb function, as well as its locomotion and ultimately its behavior, is necessary to analyze the muscles and tendons that attaches on the pathologic and neighboring area, as well as other morphological features in the skeleton.

Metatarsals and phalanges are the attachment sites of several muscle tendons of insertion that flex and extend the ankle and digits. Based on the comparisons with different myological studies on crocodilians and birds (e.g., Cracraft, 1971; Romer, 1923; Wilhite, 2003) we infer the probable muscles attachments on foot and particularly on the metatarsus II. The *extensor digitorum longus*, one of the muscles that flex the ankle and extend the digits (Schachner et al., 2011, 2020), is interpreted as inserting on the proximal dorsolateral surface (extensor surface) of the shaft of the metatarsal II, and also probably on the metatarsal III and IV, based on different statements on living crocodilians (e.g., Dilkes, 2000; Tarsitano, 1981). In crocodilians, this muscle is interpreted to insert together with the *tibialis anterior*, after merging at the ankle (Dilkes, 2000), the interpreted function of the latter muscle, is to flex the ankle joint (Schachner et al., 2011, 2020). The area of insertion of these muscles on the metatarsal II of *Bonapartesaurus* is mostly onto the pathological bone region and no particular scar is seen on it; even if these putative osteological correlates could be blurred by the pathological tissue, no scar is neither seen on the metatarsals III and IV. On the ventral (flexor) surface of the metatarsals II to IV of *Maiasaura* is reconstructed the insertion of the *gastrocnemius* (Dilkes, 2000), an important knee flexor and ankle extensor. A probable insertion site of this muscle is not possible to determine in *Bonapartesaurus* because the pes lies on the plaster block.

Bonapartesaurus, as other derived Hadrosaurinae, had a subunguligrade posture of the feet (Moreno et al., 2006), where the phalanges were mostly touching the ground and the metatarsals were more dorsally located than the phalanges, and located on top of a high footpad. This pad could have served as a cushion for an injured metatarsal, absorbing the impact from the ground. Metatarsal II is a non-major weight-bearing bone, contrasting with femora, tibia, or hip bones that have major roles in supporting the body off the ground. Thus, any injury in the latter bones can be lethal for the organism; in contrast, any injury in a non-major weight-bearing bone can usually allow (almost) normal lives (Bulstrode et al., 1986; Rothschild and Martin, 2006; Tanke and Rothschild, 2011). When deviations in structure, position, or function occur in one part of the skeleton, another part of the tends to compensate by changing its structure, position, or function, thus, injuries or malformations in one part of the organism body can provoke changes in other regions.

A putative change in *Bonapartesaurus* gait caused by the metatarsal pathology is not possible to determine with the data available. On the other hand, no abnormalities in the skeleton are observed, such as deformation on other bones or articular joints (e.g., femora, tibiae, fibulae, ilia, Cruzado-Caballero and Powell, 2017) to compensate a putative bad posture (ID-M pers. obs.). The muscles and tendons inserting onto the injured metatarsal are not the only ones performing flexion/extension of the ankle, most important movements for locomotion; consequently, the flexion/extension of the ankle and other than second digit are not that limited because other muscles and tendons, or pars of them, can assist in this movement. The data acquired and information obtained from this specimen at this moment, precludes any inference of the impact of this injury in *Bonapartesaurus* daily life.

6. CONCLUSIONS

The results obtained in the analysis of the pathologies of the caudal vertebrae and the left pes of *Bonapartesaurus*, indicate it suffered several fractures with associated infections and the presence of a neoplasm in the metatarsal II.

The traumatic accident associated with the caudal vertebra MPCA-Pv SM2/17 corresponds to an impact that leaded to the formation of a displaced fracture and a post-traumatic infection. The fracture in the vertebra MPCA-Pv SM2/19 cannot be identified as provoked by an accident, a stress event, or any other situation. The pathologies of the vertebrae may have been painful in different degrees. Based on the incomplete healing of the vertebrae fractures, we interpret that *Bonapartesaurus* death was not immediately after the accident that caused the fractures, but when the phase of resorptive reduction of the callus was still taking place. According to the tomographical data, it is considered that the metatarsal II has probably a neoplasm, but here are not enough data to assure if this lesion affects to its locomotion. This work shows that Bonapartesaurus had some lesions along its life, which could generate pain and discomfort, but they were not the direct cause of his death.

7. ACKNOWLEDGEMENTS

We thank to Diego Socolsky of the clinic Gamma Diagnostic (Tucumán),to Dra. Judith Babot for their help with CT Scan acquisition andto Sergio Llacer for his advice in trying to improve the tomographic images. We acknowledge an anonymous reviewer for his valuable comments and suggestions that have greatly improved the manuscript. This work has been partially funded by Agencia Nacional de Promoción Científica y Técnica (PICT 2016-0419; PC-C), the Universidad Nacional de Río Negro (PI 40-A-572 and PI 40-A-737; PC-C) and the Spanish Ministerio de Ciencia e Innovación and the European Regional Development Fund (CGL2017-85038-P; to PC-C).

8. REFERENCES

Alberts, B., Hopkin, K., Johnson, A.D., Morgan, D., Raff, M., Roberts, K., Walter, P. 2019. Essential cell biology. New York: W.W. Norton & Company.

Anné, J., Garwood, R.J., Lowe, T., Withers, P.J., Manning, P.L. 2015. Interpreting pathologies in extant and extinct archosaurs using micro-CT. PeerJ 3, e1130.

Anné, J., Hedrick, B.P., Schein, J.P. 2016. First diagnosis of septic arthritis in a dinosaur. Royal Society open science 3 (8), 160222.

Arbour, V.M., Currie, P.J. 2011. Tail and pelvis pathologies of ankylosaurian dinosaurs. Historical Biology 23 (4), 375-390.

Aktipis, C.A., Boddy, A.M., Jansen, G., Hibner, U., Hochberg, M.E., Maley, C.C., Wilkinson, G.S. 2015. Cancer across the tree of life: cooperation and cheating in multicellularity. Philosophical Transactions of the Royal Society B: Biological Sciences, 370 (1673): 20140219.

Bell, P.R., Coria, R. A. 2013. Palaeopathological survey of a population of *Mapusaurus* (Theropoda: Carcharodontosauridae) from the Late Cretaceous Huincul Formation, Argentina. PloS One 8 (5), e63409.

Bell, P.R., Sissons, R.L., Burns, M., Fanti, F., Currie, P. J. 2014. New saurolophine material from the upper Campanian–lower Maastrichtian Wapiti Formation, west-central Alberta. In: Eberth, D.A. and Evans, D.C. (Eds.), Hadrosaurs. Indiana University Press, Bloomington, IN, 174-190.

Bonaparte, J.F. 1984. El intercambio faunístico de vertebrados continentales entre América del Sur y del Norte a fines del Cretácico. In: Perrilliat, M.C. (Ed.), Memorias III Congreso Latinoamericano de Paleontología, Oaxtepec (Morelos, México), 438-450.

Bryant, H.N., Russell, A.P., 1992. The role of phylogenetic analysis in the inference of unpreserved attributes of extinct taxa. Philosophical Transactions of the Royal Society B: Biological Sciences 337, 405-418. https://doi.org/10.1098/rstb.1992.0117

Brett-Surman, M.K. 1979. Phylogeny and paleobiogeography of hadrosaurian dinosaurs. Nature 277, 60-562.

Cabral, U.G., Riff, D., Kellner, A.W., Henriques, D.D. 2011. Pathological features and insect boring marks in a crocodyliform from the Bauru Basin, Cretaceous of Brazil. Zoological Journal of Linnean Society 163 (suppl. 1), 140-151.

Canudo, J.I., Cruzado-Caballero, P., Moreno-Azanza, M. 2005. Possible theropod predation evidence in hadrosaurid dinosaurs from the Upper Maastrichtian (Upper Cretaceous) of Arén (Huesca, Spain). Kaupia. Darmstädter Beiträge zur Naturgeschichte 14, 9-13.

Carpenter, K. 1998. Evidence of predatory behaviour by carnivorous dinosaurs: Gaia 15.

Carrano, M.T., Hutchinson, J.R., 2002. Pelvic and hindlimb musculature of *Tyrannosaurus rex* (Dinosauria: Theropoda). Journal of Morphology 253, 207-228. https://doi.org/10.1002/jmor.10018

Cerda, I.A., Pereyra, M.E., Garrone, M., Ponce, D., Navarro, T.G., González, R., Militello, M., Luna, C.A., Jannello, J.M., 2020. A basic guide for sampling and preparation of extant and fossil bones for histological studies. Publicación Electrónica de la Asociación Paleontológica Argentina 20, 15-28.

Chhem, R., Brothwell, D.R. 2008. Paleoradiology: imaging mummies and fossils. Springer-Verlag, Berlin and Heidelberg, p. 163.

Chinsamy, A., Raath, M.A. 1992. Preparation of fossil bone for histological examination. Palaeontologia Africana 29, 39-44.

Clayton, R.J. 2018. Description of unusual pathological disorders on pubes and associated left femur from a diplodocus specimen. Paludiolan 11 (4), 179-187.

Coria, R.A., González Riga B., Casadío, S. 2012. Un nuevo hadrosáurido (Dinosauria, Ornithopoda) de la Formación Allen, provincia de la Pampa, Argentina. Ameghiniana 49, 552-572.

Cracraft, J., 1971. The Functional Morphology of the Hind Limb of the Domestic Pigeon, *Columba livia*. Bulletin of the American Museum of Natural History 4, 171-268.

Cruzado-Caballero, P. 2017. New hadrosaurid remains from the Late Cretaceous of Río Negro Province (Argentina, Late Cretaceous). Journal of Iberian Geology 43 (2), 307-318.

Cruzado-Caballero, P., Powell, J. 2017. *Bonapartesaurus rionegrensis*, a new hadrosaurine dinosaur from South America: implications for phylogenetic and biogeographic relations with North America. Journal of Vertebrate Paleontology, 37 (2), e1289381.

Cruzado-Caballero, P., Díaz-Martínez, I., Rothschild, B., Bedell, M., Pereda-Suberbiola, X. 2020. A limping dinosaur in the Late Jurassic: Pathologies in the pes of the neornithischian *Othnielosaurus consors* from the Morrison Formation (Upper Jurassic, USA). Historical Biology, DOI: 10.1080/08912963.2020.1734589

De Palma, R.A., Burnham, D.A., Martin, L.D., Rothschild, B. M., Larson, P.L. 2013. Physical evidence of predatory behaviour in *Tyrannosaurus rex*. Proceedings of the National Academy of Sciences 110 (31), 12560-12564. doi:10.1073/pnas.1216534110

De Boer, H.H., Van der Merwe, A.E., Maat, G.J.R. 2013. The diagnostic value of microscopy in dry bone palaeopathology: a review. International journal of paleopathology, 3(2), 113-121.

de Ricqlès, A., Meunier, F.J., Castanet, J., Francillon Vieillot, E. 1991. Comparative microstructure of bone. In: Hall, B.K. (Ed.), Bone, Bone Matrix and Bone Specific Products, vol. 3. CRC Press, Boca Raton, 1-78.

Díaz-Martínez, I., Pereda-Suberbiola, X., Pérez-Lorente, F., Canudo, J.I. 2015. Ichnotaxonomic review of large ornithopod dinosaur tracks: temporal and geographic implications. PloS One 10(2), e0115477.

Díaz-Martínez, I., de Valais, S., Cónsole-Gonella, C. 2016. First evidence of *Hadrosauropodus* in Gondwana (Yacoraite Formation, Maastrichtian-Danian), northwestern Argentina. Journal of African Earth Sciences 122, 79-87.

Dilkes, D.W., 2000. Appendicular myology of the hadrosaurian dinosaur *Maiasaura peeblesorum* from the Late Cretaceous (Campanian) of Montana. Transactions of the Royal Society of Edinburgh: Earth Sciences 90, 87-125. https://doi.org/10.1017/S0263593300007185

Dumbravă, M.D., Rothschild, B.M., Weishampel, D.B., Csiki-Sava, Z., Andrei, R.A., Acheson, K.A., Codrea, V. A. 2016. A dinosaurian facial deformity and the first occurrence of ameloblastoma in the fossil record. Scientific Reports 6, 29271.

Farke, A.A., Chok, D.J., Herrero, A., Scolieri, B., Werning, S. 2013. Ontogeny in the tube-crested dinosaur *Parasaurolophus* (Hadrosauridae) and heterochrony in hadrosaurids. PeerJ 1, e182.

Foth, C., Evers, S.W., Pabst, B., Mateus, O., Flisch, A., Patthey, M., Rauhut, O.W. 2015. New insights into the lifestyle of *Allosaurus* (Dinosauria: Theropoda) based on another specimen with multiple pathologies. PeerJ 3, e940.

Francillon-Vieillot, H., Buffrénil, V. de, Castanet, J., Géraudie, F., Meunier, J., Sire, J., Zylberberg, L., de Ricqlès, A.J. 1990. Microstructure and mineralization of vertebrate skeletal tissues. In: Carter, J.G. (Ed.), Skeletal Biomineralization: Patterns, Processes and Evolutionary Trends. Van Nostrand Reinhold, New York, 471e530.

García, R.A., Cerda, I.A., Heller, M., Rothschild, B.M., Zurriaguz, V. 2016 The first evidence of osteomyelitis in a sauropod dinosaur. Lethaia 50 (2), 227-236.

Gross, J., Rich, T., Vickers–Rich, P. 1993. Dinosaur bone infection. Research Explorer 9, 286-293.

Hanna, R.R. 2002. Multiple injury and infection in a sub-adult theropod dinosaur *Allosaurus fragilis* with comparisons to *Allosaurus* pathology in the Clevland-Lloyd Quarry collection. Journal of Vertebrate Paleontology 22, 76-90.

Hao, B.Q., Feng, H., Zhao, Z.Q., Ye, Y., Wan, D.X., Peng, G.Z. 2020. Different types of bone fractures in dinosaur fossils. Historical Biology, DOI 10.1080/08912963.2020.1722661.

Hearn, L., Williams, A.C.D.C. 2019. Pain in dinosaurs: what is the evidence? Philosophical Transactions Royal Society B. 374 (1785), 20190370.

Hone, D.W., Tanke, D.H. 2015. Pre-and postmortem tyrannosaurid bite marks on the remains of *Daspletosaurus* (Tyrannosaurinae: Theropoda) from Dinosaur Provincial Park, Alberta, Canada. PeerJ 3, e885.

Horner, J.R., Currie, P.J. 1994. Embryonic and neonatal morphology and ontogeny of a new species of *Hypacrosaurus* (Ornithischia, Lambeosaurinae) from Montana and Alberta. In: Carpenter, K., Hirsch, K.F., Horner, J.R. (Eds.), Dinosaur Eggs and Babies. Cambridge University Press, Cambridge, 312e336.

Horner, J.R., Weishampel, D.B., Forster, C.A. 2004. Hadrosauridae. In: Weishampel, D.B., Dodson, P., Osmólska, H. (Eds.), The Dinosauria. University of California Press, 438-463.

Hunt, T.C., Peterson, J.E., Frederickson, J.A., Cohen, J.E., Berry, J.L. 2019. First documented pathologies in *Tenontosaurus tilletti* with comments on infection in non-avian dinosaurs. Scientific Reports 9(1), 1-8.

Jacobson, E.R. (Ed.), 2007. Infectious diseases and pathology of reptiles. Viruses and viral diseases of reptiles. CRC Press, 395-460.

Jentgen-Ceschino, B., Stein, K., Fischer, V. 2020. Case study of radial fibrolamellar bone tissues in the outer cortex of basal sauropods. Philosophical Transactions of the Royal Society B, 375 (1793), 20190143.

Kappelman, J., Ketcham, R.A., Pearce, S., Todd, L., Akins, W., Colbert, M.W., Feseha, M., Maisano, J.A., Witzel, A. 2016. Perimortem fractures in Lucy suggest mortality from fall out of tall tree. Nature 537 (7621), 503.

Lü, J., Kobayashi, Y., Lee, Y.-N., Ji, Q. 2017. A new *Psittacosaurus* (Dinosauria: Ceratopsia) specimen from the Yixian Formation of western Liaoning, China: the first pathological psittacosaurid. Cretaceous Research 28, 272-276.

Mahajan, T., Ganguly, S., Para, P.A. 2015. Fracture Management in Animals: A Review. Journal of Chemical, Biological and Physical Sciences 5 (4), 4053-4057.

Matthias, A.E., McWhinney, L.A., Carpenter, K. 2016. Pathological pitting in ankylosaur (Dinosauria) osteoderms. International Journal of Paleopathology 13, 82-90.

McWhinney, L.A., Rothschild, B.M., Carpenter, K. 2001. Post-traumatic chronic osteomyelitis in *Stegosaurus* spikes. In: Carpenter, K. (Ed.), The Armored Dinosaurs. Indiana University Press, Bloomington, Indiana, 141-155.

Murphey, M.D., Choi, J.J., Kransdorf, M.J., Flemming, D.J., Gannon, F.H. 2000. Imaging of osteochondroma: variants and complications with radiologic-pathologic correlation. Radiographics 20 (5), 1407-1434.

Murphy N.L., Trexler D., Thompson M. 2006. 'Leonardo', a mummified *Brachylophosaurus* from the Judith River Formation. In: Carpenter, K. (Ed.). Horns and beaks: Ceratopsian and ornithopod dinosaurs. Indiana University Press, 117-133.

Norman, D.B., 1986. On the anatomy of *Iguanodon atherfieldensis* (Ornithischia: Ornithopoda). Bulletin de L'Institut royal des Sciences naturelles de Belgique: Sciences de la Terre 56, 281-372.

Persons, W.S., IV, Currie, P.J., 2014, Duckbills on the run: the cursorial abilities of hadrosaurs and implications for tyrannosaur-avoidance strategies. In: Eberth, D.A. and Evans, D.C. (Eds.), Hadrosaurs. Indiana University Press, Bloomington, IN, 449-458.

Peterson, J.E., Vittore, C.P. 2012. Cranial Pathologies in a Specimen of *Pachycephalosaurus*. PLoS One 7 (4), e36227. doi:10.1371/journal.pone.0036227

Pierce, B.A. 2019. Genetics: A conceptual approach. In: W.H. Freeman (Ed.), London.

Powell, J. E. 1987. Hallazgo de un dinosaurio hadrosaurido (Ornithischia, Ornithopoda) en la Formación Allen (Cretácico superior) de Salitral Moreno, Provincia de Río Negro, Argentina. In: Asociación Argentina de Geología (Ed.), Actas X Congreso Geologico Argentino. San Miguel de Tucuman (Tucuman, Argentina), 149-152.

Ramírez-Velasco, A.A., Morales-Salinas, E., Hernández-Rivera, R., Tanke, D.H. 2017. Spinal and rib osteopathy in *Huehuecanauhtlus tiquichensis* (Ornithopoda: Hadrosauroidea) from the Late Cretaceous in Mexico. Historical Biology 29 (2), 208-222.

Rega, E. 2012. Disease in dinosaurs. In: Brett-Surman, M.K., Holtz, T.R., Farlow, J.O. (Eds), The Complete Dinosaur, Indiana University Press, 666-711.

Resnick, D., Niwayama, G. 1981. Diagnosis of bone and joint disorders, Vol. 3. Philadelphia, PA: WB Saunders Co. 2058-2079.

Romer, A.S., 1923. Crocodilian pelvic muscles and their avian and reptilian homologues. Bulletin American Museum of Natural History XLVIII, 533-551.

Rothschild B.M. 2009. Scientifically rigorous reptile and amphibian osseous pathology: lessons for forensic herpetology from comparative and paleo–pathology. Applied Herpetology 6 (1), 47-79.

Rothschild, B.M., Martin, L.D. 2006. Skeletal impact of disease. In: Lucas, S.G., Hutnt, A.P., Morgan, G.S., Spielmann, J.A., Zeigler, K.E., Wit, R. (Eds.). Bulletin New Mexico Museum of Natural History and Science 33, 1-226.

Rothschild, B.M., Molnar, R.E. 2005. Sauropod stress fractures as clues to activity. In: Tidwell, V., Carpenter, K. (Eds.). Thunder-lizards: the Sauropodomorph Dinosaurs. Indiana University Press, 381-392.

Rothschild, B.M., Tanke, D.H. 2006. Osteochondrosis in Late Cretaceous Hadrosauria: a manifestation of ontologic failure. In: Carpenter, K. (Ed.). Horns and beaks: Ceratopsian and ornithopod dinosaurs. Indiana University Press, 171-183.

Rothschild, B.M., Schultze, H.P., Pellegrini, R. (Eds.) 2012. Herpetological Osteopathology: Annotated bibliography of amphibians and reptiles. New York: Springer Science.

Salgado, L., Azpilicueta, C. 2000. Un nuevo saltasaurino (Sauropoda, Titanosauridae) de la provincia de Río Negro (Formacíon Allen, Cretácico Superior), Patagonia, Argentina. Ameghiniana 37 (3), 259-264.

Schachner, E.R., Irmis, R.B., Huttenlocker, A.K., Sanders, K., Cieri, R.L., Nesbitt, S.J., 2020. Osteology of the Late Triassic Bipedal Archosaur *Poposaurus gracilis*

(Archosauria: Pseudosuchia) from Western North America. The Anatomical Record 303, 874-917. https://doi.org/10.1002/ar.24298

Schachner, E.R., Manning, P.L., Dodson, P., 2011. Pelvic and hindlimb myology of the basal archosaur *Poposaurus gracilis* (Archosauria: Poposauroidea). Journal of Morphology 272, 1464-1491. https://doi.org/10.1002/jmor.10997

Senter, P., Juengst, S.L. 2016. Record-breaking pain: the largest number and variety of forelimb bone maladies in a theropod dinosaur. PloS One 11 (2), e0149140.

Siviero, B.C., Rega, E., Hayes, W.K., Cooper, A.M., Brand, L.R., Chadwick, A.V. 2020. Skeletal trauma with implications for intratail mobility in *Edmontosaurus annectens* from a monodominant bonebed, lance formation (Maastrichtian), Wyoming USA. Palaios 35 (4), 201-214.

Straight, W.H., Davis, G.L., Skinner, H.C.W., Haims, A., McClennan, B.L., Tanke, D. H. 2009. Bone lesions in hadrosaurs: Computed Tomographic Imaging as a guide for paleohistologic and stable-isotopic analysis. Journal of Vertebrate Paleontology 29 (2), 315-325.

Sullivan, R.M., Tanke, D.H., Rothschild, B.M. 2000. An impact fracture in an ornithomimid (Ornithomimosauria: dinosauria) metatarsal from the Upper Cretaceous (Late Campanian) of New Mexico. Bulletin New Mexico Museum of Natural History and Science 17, 109-111.

Tanke, D.H., Farke, A.A. 2006. Bone resorption, bone lesions, and extracranial fenestrae in ceratopsid dinosaurs: a preliminary assessment In: Carpenter, K. (Ed.). Horns and beaks: Ceratopsian and ornithopod dinosaurs. Indiana University Press, 319-347.

Tanke, D.H., Rothschild, B.M. 2014. Paleopathology in Late Cretaceous Hadrosauridae from Alberta, Canada with comments on a putative *Tyrannosaurus* bite injury on an *Edmontosaurus* tail. In: Eberth, D.A. and Evans, D.C. (Eds.), Hadrosaurs. Indiana University Press, Bloomington, IN, 540-572.

Tarsitano, S.F., 1981. Pelvic and hindlimb musculature of archosaurian reptiles (Unpubl. PhD thesis). The City University of New York,191 pp.

Waldron, T. (Ed.) 2009. Paleopathology. New York: Cambridge University Press.

Weiss, E. (Ed.) 2014. Paleopathology in perspective: Bone health and disease through time. Rowman & Littlefield.

Witmer, L.M., 1997. The evolution of the antorbital cavity of archosaurs: A study in soft-tissue reconstruction in the fossil record with an analysis of the function of pneumaticity. Journal of Vertebrate Paleontology 17, 1-76. https://doi.org/10.1080/02724634.1997.10011027

Witmer, L.M., 1995. The extant phylogenetic bracket and the importance of reconstructing soft tissues in fossils. In: Thomason, J.J. (Ed.), Functional Morphology in Vertebrate Paleontology. Cambridge University Press, 19-33.

Xing, L., Bell, P. R., Rothschild, B. M., Ran, H., Zhang, J., Dong, Z.-M. Zhang, W., Currie, P.J. 2013. Tooth loss and alveolar remodeling in *Sinosaurus triassicus* (Dinosauria: Theropoda) from the Lower Jurassic strata of the Lufeng Basin, China. Chinese Science Bulletin 58 (16), 1931-1935.

Xing, L.D., Rothschild, B.M., Randolph-Quinney, P.S., Wang, Y., Parkinson, A.H., Ran, H. 2018. Possible bite-induced abscess and osteomyelitis in *Lufengosaurus*

(Dinosauria, Sauropodomorph) from the Lower Jurassic of the Yimen Basin, China. Scientific Report 8, 5045.

Figure captions:

Figure 1. Map showing the location of the Salitral Moreno site (General Roca, Río Negro, Argentina).

Figure 2. *Bonapartesaurus rionegrensis* pathological bones. A, B and E, MPCA-Pv SM2/17, mid-caudal vertebra; C, D, and F, MPCA-Pv SM2/19, mid-caudal vertebra; G and H, MPCA-Pv SM2/60-69, left pes. A, C, E, F, and H, lateral views; B, ventral view and D and G, dorsal view. E, and F, details of the pathologic surfaces of the vertebrae neural spines. Black rectangle indicates the pathological areas, the arrows the location of the pathologies, and the black star the area where the histological sample was taken. Scale bar equals 5 cm in A-D and 2 cm in E and F.

Figure 3. *Bonapartesaurus rionegrensis* mid-caudal vertebra, MPCA-Pv SM2/17. B-G, sequence of CT scan images in serial axial section from the distal end of the neural spine (B) to the middle region (G). B, non-pathologic section. C-G, pathologic sections including white areas due to resins (marked with an arrow in C). Black lines mark the locations of the CT scan images. Scale bar equals 5 cm in A and 1 cm in B-G.

Figure 4. *Bonapartesaurus rionegrensis* mid-caudal vertebra, MPCA-Pv SM2/19. B-F, sequence of CT scan images in serial axial section from the distal end of the neural spine (B) to the middle region (F). B, non-pathologic section. C-E, pathologic area including white areas due to resins (marked with an arrow in E). C and D, can sense a thin original cortex. F, non-pathologic bone section. Black lines mark the location of the CT scan images. Scale bar equals 5 cm in A and 1 cm in B-F.

Figure 5. *Bonapartesaurus rionegrensis* left pes, MPCA-Pv SM2/60-69, sequence of CT scan images (B and C) in dorsal view of the complete pes and (D-I) in serial axial section of the tumoural tissue of the metatarsal II, from proximal region (D) to the distal one (I). B, dorsal view of the pes, note the metallic bar. C, detail of the metatarsal II in dorsal view showing the periosteal reaction and the reduction in bone density in the diaphysis. D-I, show the non-uniform distribution of the periosteal reaction. E, the arrow marks areas of cortical destruction. G-I, the arrows mark the burst of the osseous tissue through the cortex. Black lines mark the locations of the CT scan images. Scale bar equal 2 cm in D-I.

Figure 6. Bone histology of pathological metatarsal II of *Bonapartesaurus rionegrensis* MPCA SM2/60-69. A, general view of the complete section. Black arrowheads indicate the boundaries between pathological (upper portion of the sample) and non-pathological (lower portion) bone tissues. B-D, Pathological bone tissue under different magnification. Note the high density and irregular shape of osteocyte lacunae in D. E and F, Large resorption cavities (rc) in the pathological region. The cavities exhibit irregular shape and are partially coated with secondary lamellar bone tissue (slb). G, transition between pathological bone tissue (upper region) and non-pathological (lower region). H, Dense Haversian bone tissue of the non-pathological area. Remains of unremodelled primary bone tissue (upb) in some areas. A, B, D, E, and G, plane polarized light. C, F, and H, cross-polarized light with lambda compensator.

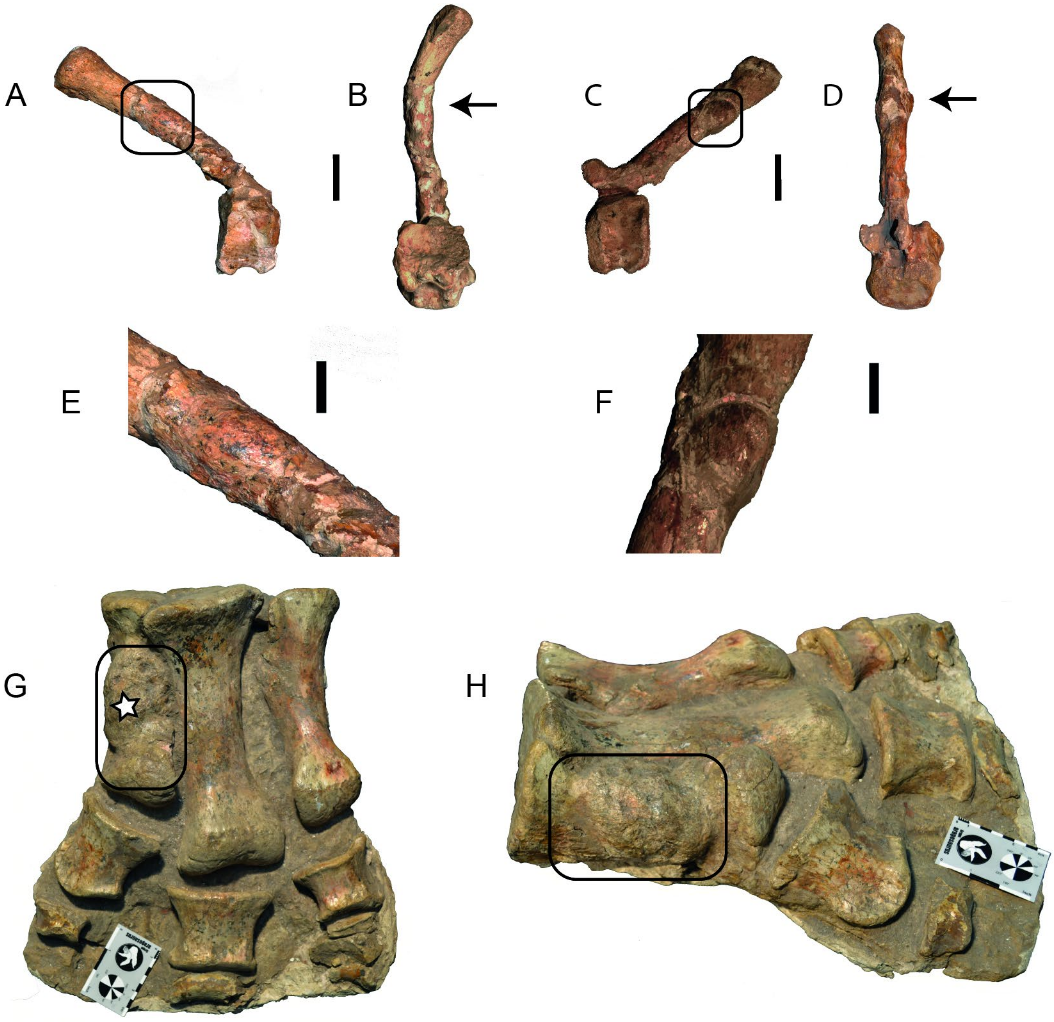

721

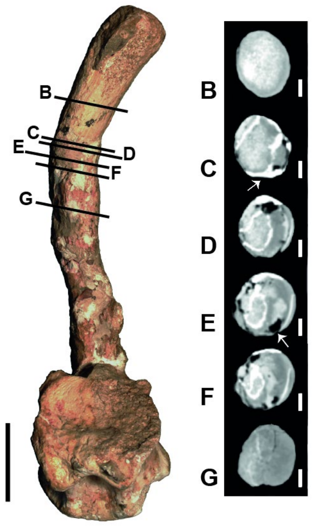

722

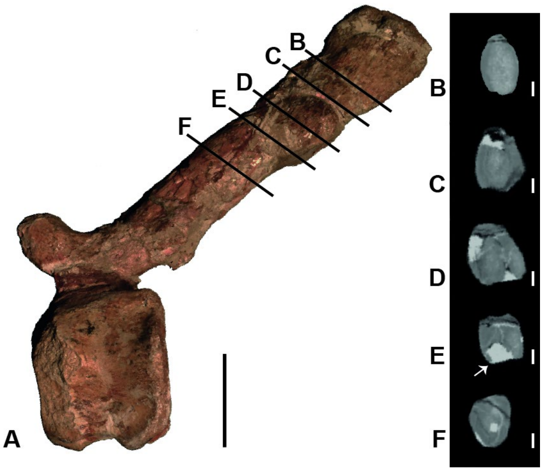

A
B
C
D
E
F

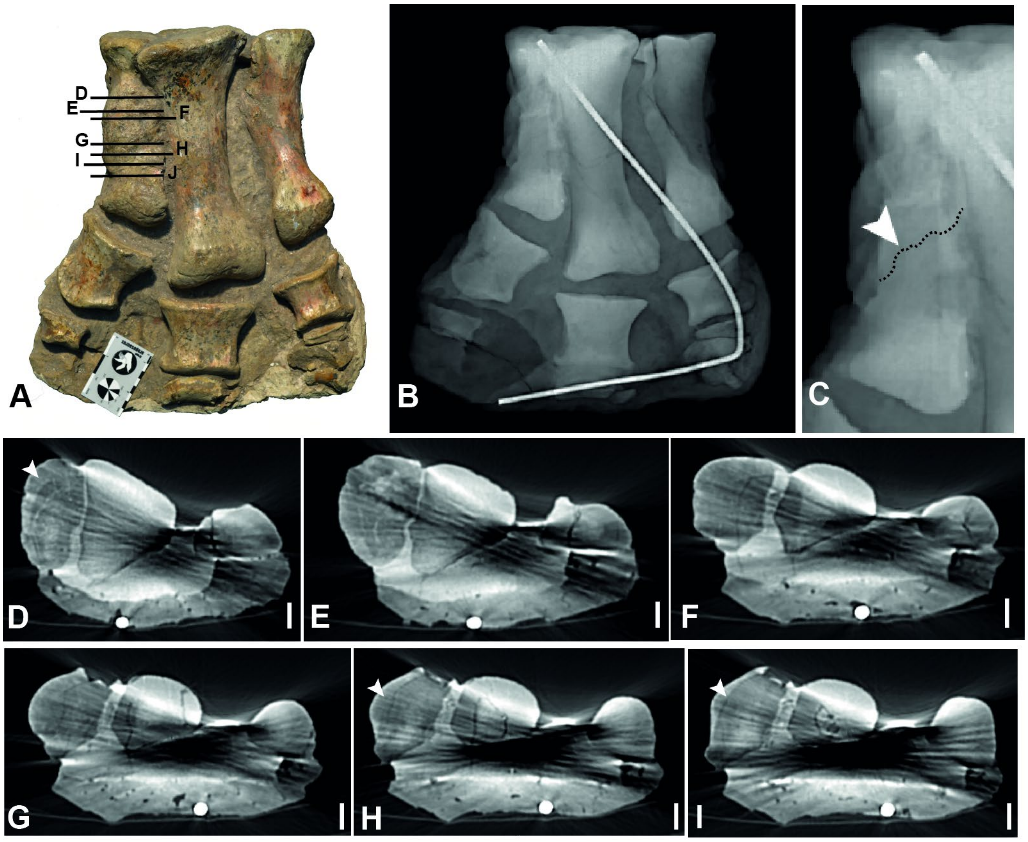

A
B
C
D
E
F
G
H
I
J

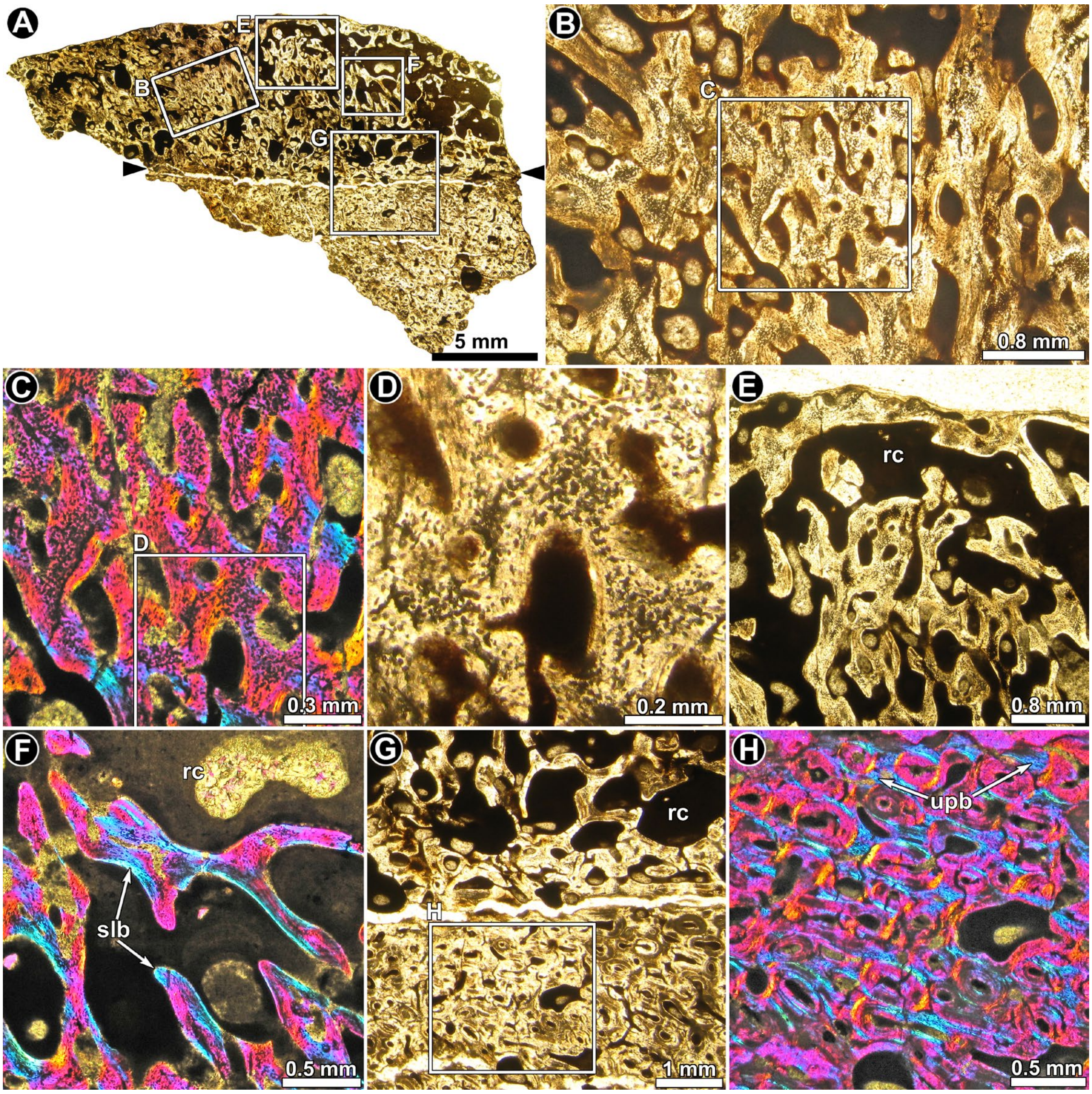
A
B
C
D
E
F
G
H
5 mm
0.8 mm
0.3 mm
0.2 mm
0.8 mm
rc
slb
rc
0.5 mm
rc
1 mm
upb
0.5 mm